

Study of Trajectory of Spin-Stabilised Artillery Projectiles

M. Krishnamurthy, D.G. Wakankar* and R. Sankar**

*Experimental Aerodynamics Division, National Aeronautical Laboratory
Bangalore-560 017*

ABSTRACT

Equations of motion for conventional spin-stabilised artillery projectile have been derived using a pseudo-stability axes system in addition to body-fixed and space-fixed axes systems. The aerodynamic forces and moments have been represented by their respective coefficients and the effects of Mach number and Reynolds number have been suitably accounted. The magnus terms which are significant at high rates of spin are estimated using a simple model. The set of equations have been partly linearised and solved numerically for a typical projectile using NAG system routines. Various trajectory parameters are computed and compared with the range-table data for the projectile. A parametric study has been carried out varying the aerodynamic coefficients to understand the sensitivity of the results obtained.

1. INTRODUCTION

In the history of warfare, the success or failure of a land battle can invariably be traced to the effective use or otherwise of artillery, and conventional spin-stabilised projectiles continue to be a major 'weapon' of the artillery world. On the battlefield of 1990s effective use of artillery would demand first round hit capability; quick switching of guns from one target to another; and extremely fast reaction to meet the

Received 6 December 1989, revised 23 March 1990

* *Military Secretary's Branch, Army HQ, New Delhi-110 011*

** *Computer Science Department, University of Poona, Pune-411 007*

requirements of highly mobile battles. These demands can be met by fast acquisition of the target, accurate computation of the gun data after accounting for all the known nonstandard conditions, and an equally efficient means of delivering the rounds on the target. The gun data computation using the tabulated data in the range-tables is a highly inefficient approach though commonly used by many countries. The process is manual, time consuming, involves interpolation errors and requires repetitive work for each firing. With the availability of sophisticated computers it should be possible to compute the complete gun data more accurately in a shorter time eliminating the possible human errors, thus achieving more effective neutralisation of the target.

The present work reports a general mathematical model developed to describe the motion of a spin-stabilised axisymmetric projectile and the resulting equations of motion which have been numerically solved to yield the complete trajectory of the projectile. The aerodynamic forces and moments are represented in terms of the corresponding coefficients and the effects of Reynolds and Mach numbers are suitably accounted. The Magnus terms which are significant at high rates of spin are incorporated based on a simple model. The method can give improved accuracy of predicting the point of fall and can be applied to any projectile of known aerodynamic characteristics.

2. EQUATIONS OF MOTION

Six-degree equations of motion for the projectile have been written making use of three systems of coordinate axes (Fig.1), viz space-fixed axes, body fixed axes, and an intermediate pseudo-stability axes. In the pseudo-stability axes system Y-axis always lies in the initial $X_0 Y_0$ plane and is not allowed to roll¹. The rigid-body linear and angular momentum equations for the projectile are written in the space-fixed coordinate system first, and are then transferred to body-fixed coordinate system, using the Eulerian angles—angle of yaw ψ , angle of pitch θ , and angle of roll ϕ —representing the orientation of the projectile in space. The effect of rotation of

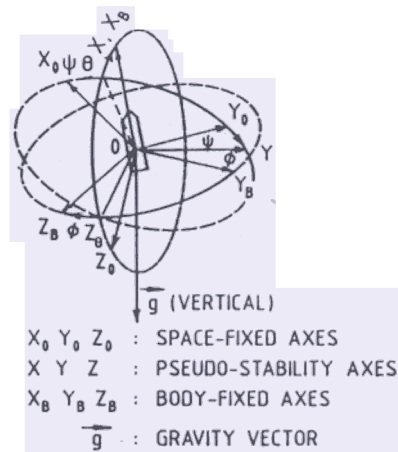


Figure 1. Axes system.

body-axes and pseudo-stability axes on the inertial terms are accounted for using Poisson's formula. The external forces include gravitational force and aerodynamic forces and moments. The details of the derivation are presented by Wakankar² (steps involved are outlined in the Appendix).

2.1 Aerodynamic Forces and Moments

The aerodynamic forces and moments are expressed in coefficient forms as

$$F_{AX_B, Y_B, Z_B} = \frac{1}{2} \rho V^2 S C_{X,Y,Z}$$

$$M_{X_B, Y_B, Z_B} = \frac{1}{2} \rho V^2 S l C_{l,m,n} \tag{1}$$

where, the subscripts X, Y, Z represent components along and about X, Y and Z axes, and l, m and n are the rolling, pitching and yawing moment components. C is the force or moment coefficient, V the projectile speed, ρ the surrounding air density and S and l are the reference area and length of the projectile respectively. Any aerodynamic force or moment coefficient in Eqn (1) can be, in general, expressed as :

$$C_a = C_{a0} + C_{a\alpha} \alpha + C_{a\beta} \beta + C_{a\dot{\alpha}} \left(\frac{\dot{\alpha}l}{2V} \right) + C_{a\dot{\beta}} \left(\frac{\dot{\beta}l}{2V} \right)$$

First order aerodynamic terms

$$+ C_{ap} \left(\frac{pl}{2V} \right) + C_{aq} \left(\frac{ql}{2V} \right) + C_{ar} \left(\frac{rl}{2V} \right)$$

$$+ C_{a\dot{\alpha}p} \alpha \left(\frac{pl}{2V} \right) + C_{a\dot{\beta}p} \beta \left(\frac{pl}{2V} \right) + C_{a\dot{\alpha}p} \left(\frac{\dot{\alpha}l}{2V} \right) \left(\frac{pl}{2V} \right) + C_{a\dot{\beta}p} \left(\frac{\dot{\beta}l}{2V} \right) \left(\frac{pl}{2V} \right)$$

Magnus terms

$$+ C_{app} \left(\frac{pl}{2V} \right)^2 + C_{aqp} \left(\frac{ql}{2V} \right) \left(\frac{pl}{2V} \right) + C_{arp} \left(\frac{rl}{2V} \right) \left(\frac{pl}{2V} \right)$$

+ higher order terms

(2)

where, p, q and r are the roll, pitch and yaw rates of the projectile (expressible in terms of ψ, θ and φ and their time derivatives); α and β are the angles of attack and side slip. The second and third subscripts represent derivatives with respect to the corresponding nondimensional variable, and (•) represents time derivative. The second order terms retained in Eqn (2) are the Magnus terms and are significant for large spin rates. The coefficients C_a are assumed to be independent of the motion variables and are only functions of flight Mach and Reynolds numbers. For bodies possessing 90° rotational symmetry, the following simplifications can be made for the coefficients :

$$C_{X\alpha} = C_{X\beta} = C_{X\dot{\alpha}} = C_{X\dot{\beta}} = C_{Xp} = C_{Xq} = C_{Xr} = 0$$

$$C_{Y\dot{\alpha}} = C_{Z\dot{\alpha}} = C_{Y\dot{\beta}} = C_{Z\dot{\beta}} = C_{Y\dot{p}} = C_{Z\dot{p}} = C_{Y\dot{q}} = C_{Z\dot{q}} = C_{Y\dot{r}} = C_{Z\dot{r}} = C_{Yq} = C_{Zq} = C_{Yr} = C_{Zr} = C_{Yp} = C_{Zp} \tag{3}$$

$$\begin{aligned}
C_{l_0} &= C_{l\alpha} = C_{l\beta} = C_{l\dot{\alpha}} = C_{l\dot{\beta}} = C_{l_q} = C_{l_r} = 0 \\
C_{m_0} &= C_{n_0} = C_{m\beta} = C_{n\alpha} = C_{m\dot{\beta}} = C_{n\dot{\alpha}} = C_{m_p} = C_{n_p} = C_{m_r} = C_{n_q} = 0 \\
C_{Y\beta} &= C_{Z\alpha}; C_{Y\dot{\beta}} = C_{Z\dot{\alpha}}; C_{Y_r} = -C_{Z_q}; C_{m\alpha} = -C_{n\beta}; C_{m\dot{\alpha}} = -C_{n\dot{\beta}}; C_{m_q} = C_{n_r} \\
C_{X\alpha\phi} &= C_{X\beta\phi} = C_{X\dot{\alpha}\phi} = C_{X\dot{\beta}\phi} = C_{X_{qp}} = C_{X_{rp}} = 0 \\
C_{Y\beta\phi} &= C_{Z\alpha\phi} = C_{Y\dot{\beta}\phi} = C_{Z\dot{\alpha}\phi} = C_{Y_{pp}} = C_{Z_{pp}} = C_{Y_{rp}} = C_{Z_{rp}} = 0 \\
C_f &= 0 \\
C_{m\alpha\phi} &= C_{n\beta\phi} = C_{m\dot{\alpha}\phi} = C_{n\dot{\beta}\phi} = C_{m_{pp}} = C_{n_{pp}} = C_{m_{qp}} = C_{n_{rp}} = 0 \\
C_{Y\alpha\phi} &= -C_{Z\beta\phi}; C_{Y\dot{\alpha}\phi} = -C_{Z\dot{\beta}\phi}; C_{Y_{qp}} = C_{Z_{rp}}; C_{m\beta\phi} = C_{n\alpha\phi}; C_{m\dot{\beta}\phi} = C_{n\dot{\alpha}\phi}; C_{m_{rp}} = -C_{n_{qp}}
\end{aligned} \tag{3}$$

2.2 Linearisation and Nondimensional Equations

Variables α , β , ψ , q and r are initially zero and are assumed to be small during the trajectory so that the equations can be linearised in these variables by ignoring the higher order terms. Variables V , θ and p are not small and the nonlinear terms in V and θ are retained. However, variation in p over the initial spin rate p_0 can be assumed to be small and linearisation can be carried out in the variable $(p-p_0)$. Equations are nondimensionalised using

$$u = \frac{V}{V_0}; \quad t^+ = \frac{t}{\tau}; \quad \tau = \frac{l}{V_0}; \quad D = \frac{d}{dt^+} \tag{4}$$

where V_0 is the muzzle velocity and t is the real-time, and they are given below in the final form :

$$\begin{aligned}
Du - u\alpha D\alpha - u\beta D\beta + u\alpha D\theta - [u\beta \cos \theta - K_1 C_{X_{rp}} E_0 \sin \theta] D\psi \\
- K_1 C_{X_{rp}} E_0 D\phi = K_1 u^2 C_{X_0} - K_1 C_{X_{rp}} E_0^2 - K \sin(\gamma_0 + \theta)
\end{aligned} \tag{5}$$

$$\begin{aligned}
\beta Du + \left[u - \frac{K_1}{2} u C_{Y_\beta} \right] D\beta - \frac{K_1}{2} E_0 C_{Y_{\dot{\alpha}}} D\alpha - \frac{K_1}{2} E_0 C_{Y_{\dot{\beta}}} D\theta \\
+ \left[u \cos \theta \left(1 - \frac{K_1}{2} C_{Y_r} \right) \right] D\psi = K_1 u^2 C_{Y_\beta} \beta + K_1 u \alpha E_0 C_{Y_{\dot{\alpha}}} + K \psi \sin \gamma_0
\end{aligned} \tag{6}$$

$$\begin{aligned}
\alpha Du + \left[\frac{K_1}{2} u C_{Z_\alpha} \right] D\alpha - \frac{K_1}{2} E_0 C_{Z_{\dot{\beta}}} D\beta - \left[u \left(1 + \frac{K_1}{2} C_{Z_q} \right) \right] D\theta \\
\frac{K_1}{2} C_{Z_{rp}} E_0 \cos \theta D\psi = K_1 u^2 \alpha C_{Z_\alpha} + K_1 u \beta E_0 C_{Z_{\dot{\beta}}} + K \cos(\gamma_0 + \theta)
\end{aligned} \tag{7}$$

where

$$u = \frac{V}{V_0}, \quad K_1 = \frac{\rho S l}{2m}, \quad K = \frac{g l}{V_0^2}, \quad E_0 = \frac{p_0 l}{2V_0}$$

$$D^2 \phi - \sin \theta D^2 \psi = K_2 u C_{1p} (D\phi - \sin \theta D\psi) \quad (8)$$

$$D^2 \theta + E_0 \cos \theta \left[\frac{2I_{XB}}{I_{YB}} - K_3 C_{m\dot{p}} \right] D\psi - K_3 u C_{m\dot{\alpha}} D\alpha - K_3 u C_{m\dot{\theta}} D\theta - K_3 E_0 C_{m\dot{\beta}} D\beta = 2K_3 u^2 C_{m\alpha} \alpha + 2K_3 u \beta E_0 C_{m\dot{\beta}} \quad (9)$$

$$\cos \theta D^2 \psi - \left[E_0 \left(\frac{2I_{XB}}{I_{ZB}} + K_3 C_{n\dot{p}} \right) \right] D\theta - K_3 u C_{n\dot{\beta}} D\beta - K_3 u \cos \theta C_{n\dot{\psi}} D\psi - K_3 E_0 C_{n\dot{\alpha}} D\alpha = 2K_3 u^2 \beta C_{n\beta} + 2K_3 u \alpha E_0 C_{n\dot{\alpha}} \quad (10)$$

where

$$K_2 = \frac{\rho S l^3}{4I_{XB}}; \quad K_3 = \frac{\rho S l^3}{4I_{YB}} = \frac{\rho S l^3}{4I_{ZB}}$$

g is the acceleration due to gravity, m the mass of the projectile and I its moment of inertia.

The kinematic equations relating the velocity components along $X_0 Y_0 Z_0$ to the motion variables are given in the nondimensional form by

$$DX_0 = u l (\cos \theta + \alpha \sin \theta) \quad (11)$$

$$DY_0 = u l (\psi \cos \theta + \beta) \quad (12)$$

$$DZ_0 = u l (-\sin \theta + \alpha \cos \theta) \quad (13)$$

The initial conditions for Eqns (5) to (13) are,

$$\text{at } t^+ = 0; \quad u = 1; \quad \dot{\phi} = p_0$$

$$\alpha = \beta = \theta = \phi = \psi = \dot{\theta} = \dot{\psi} = 0; \quad \text{and } X_0 = Y_0 = Z_0 = 0 \quad (14)$$

2.3 Solution

The set of Eqns (5) to (13) has been numerically solved on DEC-10 computer at IIT, Kanpur using Gear's variable-order-variable-step routine³ for a typical projectile for which aerodynamic data was partly available. All the first order aerodynamic coefficients except drag coefficient have been computed as per USAF Stability and Control Datcom method⁴ and the compressibility effects have been accounted using similarity rules⁵. The drag coefficient has been computed for different Mach numbers and Reynolds numbers⁶. The Magnus coefficients have been estimated

assuming a two-dimensional flow in the cross-flow plane². The temperature and density variations are chosen to correspond to ICAO atmosphere. The physical parameters of the trajectory shown in Fig. 2, viz range and height have been computed from the equations

$$\text{Range} = \sqrt{X_0^2 \cos^2 \gamma_0 + Y_0^2 + Z_0^2 \sin^2 \gamma_0 + X_0 Z_0 \sin 2\gamma_0} \quad (15)$$

$$\text{Height} = X_0 \sin \gamma_0 - Z_0 \cos \gamma_0 \quad (16)$$

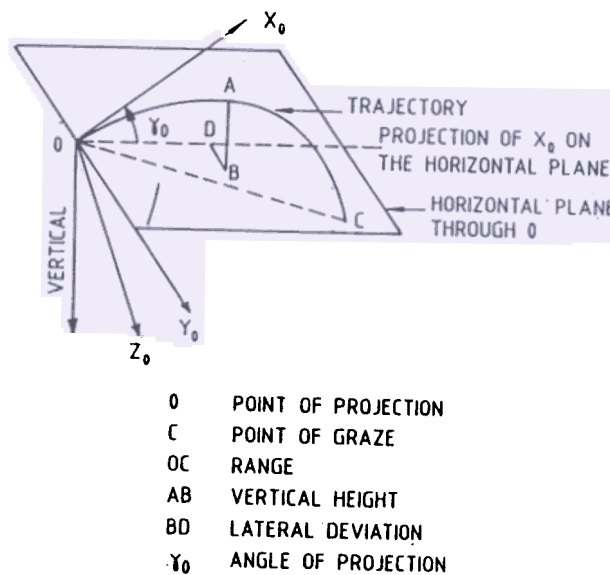


Figure 2. Geometry of the trajectory.

A parametric study has been carried out by varying the aerodynamic coefficients one at a time to study the sensitivity of the results to these coefficients.

3. RESULTS AND DISCUSSION

3.1 Trajectories

Results have been computed for a muzzle velocity of 297 m/s and for angles of projection of 15, 25 and 30°, and are presented in Figs. 3 to 6. The initial spin rate is related to the muzzle velocity for a given gun and is accordingly set. The program takes on an average a CPU time of 3 to 4 s to execute a complete trajectory and write all the parameters at 1000 intermediate stations. In Fig. 3, the computed trajectories for the measured as well as theoretically estimated drag coefficients are presented and are compared with range-table data for three values of γ_0 . The computed trajectories for the two drag coefficients are quite close to each other, but they deviate

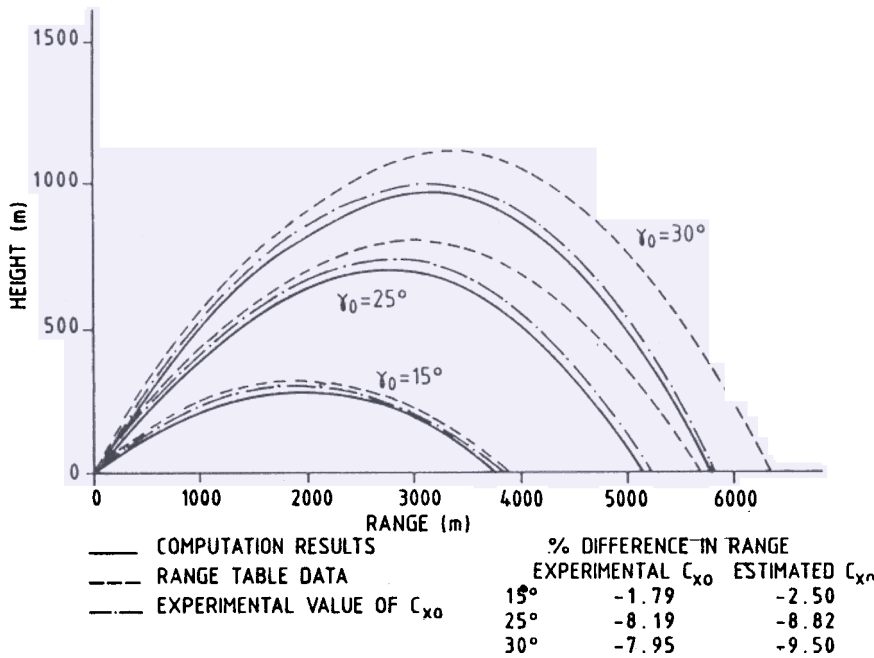


Figure 3. Height vs range; muzzle velocity = 297 m/s, $p_0 = 935.39$ rad/s.

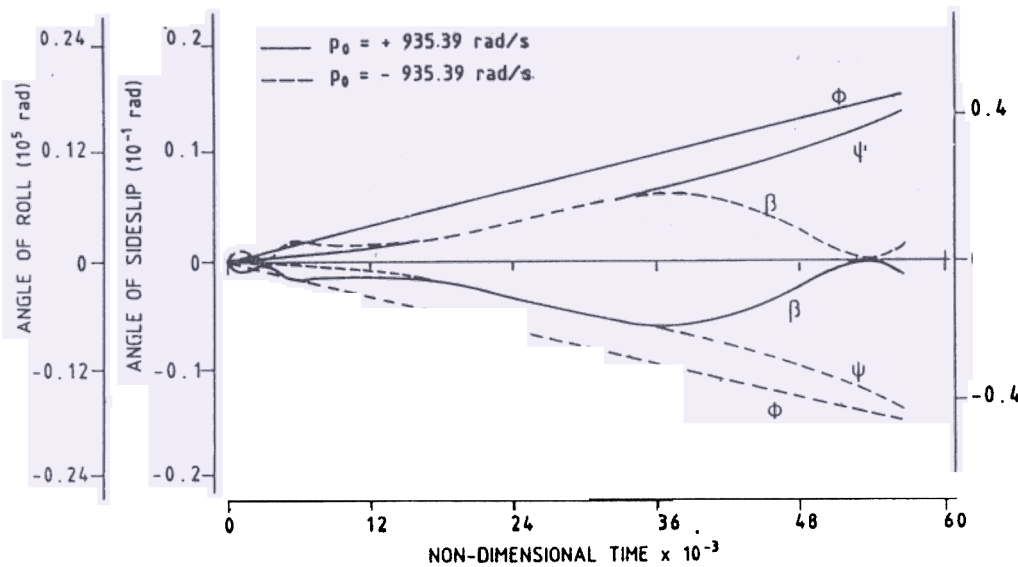


Figure 4. Time histories of lateral parameters, muzzle velocity = 297 m/s, $\gamma_0 = 25^\circ$.

considerably from the range-table plots for $\gamma_0 = 25$ and 30° . This difference builds up significantly during the second half of the trajectory and increases with increase of γ_0 initially. The computed results predict lower values of range and height than those of range-table results. Percentage deviation in range between the computed and range-table results are also presented in Fig. 3.

Figure 4 shows the time histories of the lateral parameters β , ψ and ϕ for a complete trajectory. It is observed that angle of yaw and roll angle build up continuously over the trajectory while the sideslip angle undergoes fluctuations. Similarly, it was observed in the case of longitudinal variables², that while pitch angle builds up continuously (negatively) with time, the angle of attack exhibits fluctuating variations. It was further noticed that θ variation with time is almost linear so that $\dot{\theta}$ can be approximated to zero for simplifying the model. Variation of ϕ with time in Fig. 4 is also seen to be almost linear implying that variation in spin rate is negligible. It is observed that the sideslip angle β remains small throughout the trajectory, so also the longitudinal parameter² a . These results justify the *a priori* assumption of small a , β , q and $(p - p_0)$. However, assumption of small ψ and hence small r seems to be in doubt from the observed results.

3.2 Effect of Magnus Terms

The influence of Magnus terms on the trajectory are shown in Figs. 5 and 6. In Fig. 5, variations of angle of attack and sideslip angle with time are presented with and without Magnus terms taken into consideration. In the absence of Magnus effect both α and β show variation with large fluctuations. While the angle of attack seems to settle down to a small steady state value in the later part of the trajectory, the sideslip angle still retains a large value at the end of the trajectory. The angle of attack variation with Magnus terms included is less fluctuating as compared to the variation without Magnus terms. This smoothing of the variation due to Magnus terms is even more pronounced in the case of sideslip angle variation. In Fig. 6, the significant influence of the Magnus terms on the lateral deviation Y_0 , has been presented. It is

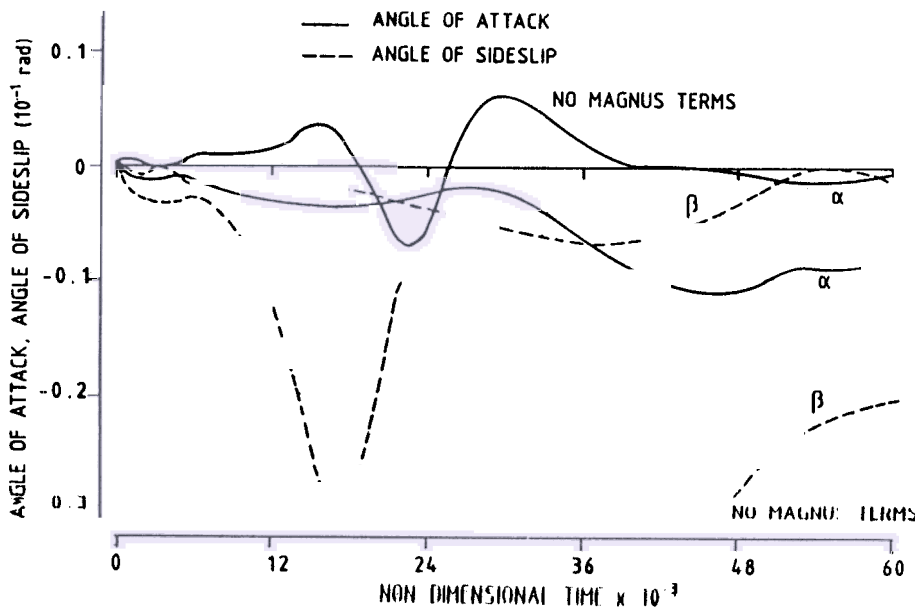


Figure 5. Effect of Magnus terms, muzzle velocity = 297 m/s, $p_0 = 935.39$ rad/s, $\gamma_0 = 25^\circ$.

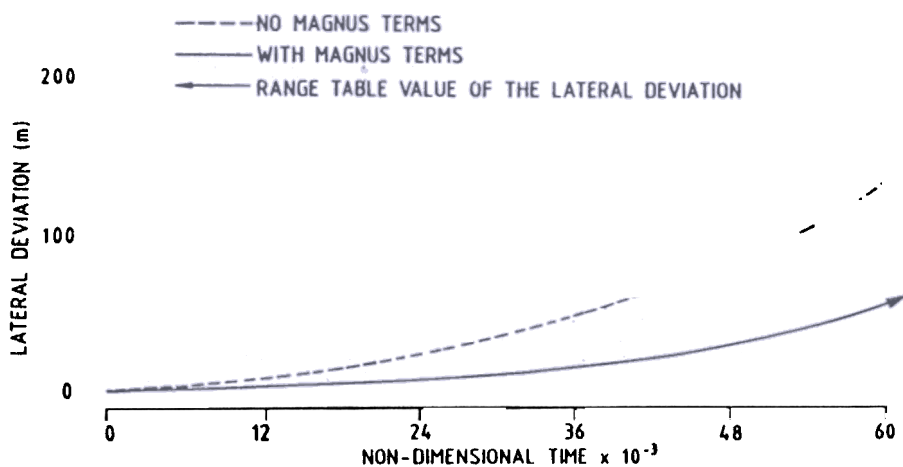


Figure 6. Effect of Magnus terms on lateral deviation ; muzzle velocity = 297 m/s, $p_0 = 935.39$ rad/s, $\gamma_0 = 25^\circ$.

noticed that while the lateral deviation builds up gradually along the trajectory for both the cases, the Magnus effect brings down the magnitude of the lateral deviation considerably, and the value of Y_0 with the Magnus effect included is very close to the range-table data for the particular case studied here. This emphasises the need to include the Magnus effect terms in the analysis.

3.3 Parametric Study

Figure 7 shows the dependence of range and height on the drag coefficient C_{x0} . It is seen that a reduction in drag coefficient results in increase of range and height and vice versa. At lower drag coefficient, the changes are more than those at higher

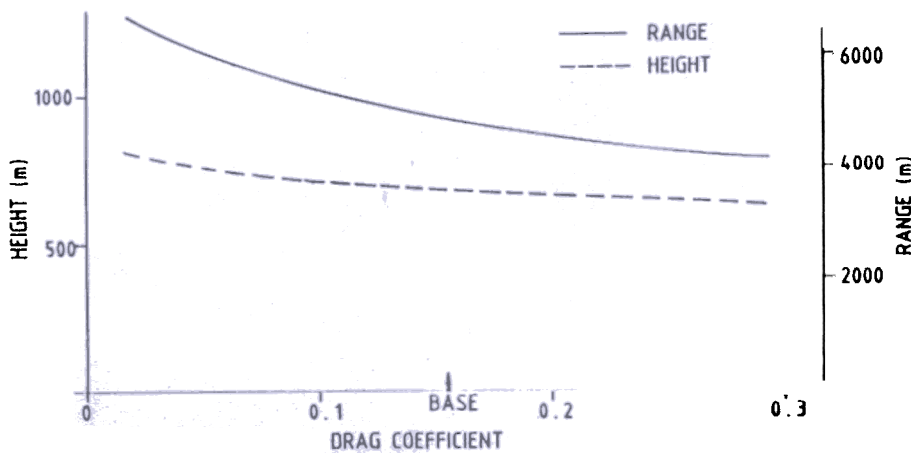


Figure 7. Effect of variation of the drag coefficient; muzzle velocity = 297 m/s, $p_0 = 935.39$ rad/s, $\gamma_0 = 25^\circ$